

Gustav K. von Schulthess, M.D., Ph.D.
Charles B. Higgins, M.D.

Blood Flow Imaging with MR: Spin-Phase Phenomena¹

Blood flow phenomena occurring when flow is within the magnetic resonance (MR) imaging plane were analyzed. In this situation, the signal intensity of vascular lumina is predominantly determined by spin-phase change phenomena, and section transition effects of moving spins can be neglected. In this paper, we develop the concepts of in-plane flow, with emphasis on the notion that the spatial variations in velocity and acceleration of blood, which mainly occur along vessel walls, are important determinants of intravascular signal loss in MR images. Flow patterns in the large mediastinal arteries were qualitatively and quantitatively analyzed in six healthy subjects and 14 patients with hemodynamic abnormalities using multiple electrocardiograph-gated image acquisition; ungated studies of 30 patients were analyzed for venous flow effects. Intraluminal signal was strongly dependent on the phase of the cardiac cycle and the echo number. Signal loss was found to occur along vessel walls, in vascular bends, and at bifurcations.

Index terms: Blood, flow dynamics • Blood vessels, magnetic resonance studies, 96.129 • Magnetic resonance, technology

Radiology 1985; 157:687-695

BLOOD vessels usually produce little signal on magnetic resonance (MR) images, but vascular lumina sometimes exhibit high, rather than low, signal intensity. It is important to understand in which physiologic and pathologic circumstances this occurs so that intravascular signal can be recognized as such.

MR holds great potential for the imaging of blood flow (1-11). Specifically, the exquisite sensitivity of some MR pulse sequences to motion suggests that MR imaging may be used to investigate and diagnose diseases such as atherosclerosis, since it has been suggested that abnormal arterial flow patterns, resulting in increased shear forces on the vessel wall, predispose to the development of atherosclerotic plaques (12). Thus, MR imaging may become a versatile and accurate tool with which to study blood flow, making it an excellent imaging modality to depict not only healthy and diseased anatomy, but also cardiovascular physiology and pathophysiology.

It is becoming apparent that many factors combine to affect the regional intensity of flowing blood on MR images. Not all are operative on every occasion, and in some instances, one factor predominates. The signal from blood depends on, and changes with, the following factors, which can be grouped as flow factors and MR imaging factors. Flow factors include the direction of flow; the motion characteristics (velocity, acceleration, etc.), which depend strongly on the phase of the cardiac cycle; and the flow profile (i.e., the spatial distribution of velocities and accelerations across the lumen of the vessel). MR imaging-related factors include the pulse sequence (i.e., spin echo and inversion recovery, characterized by echo time, repetition time, and inversion time), the position of a section in two-dimensional multisection imaging, the spin-echo type (odd or even), and the spatial direction and type of imaging gradients (i.e., linear gradients). Finally, it is important whether a study is acquired in an untriggered or electrocardiograph-gated (ECG-gated) mode.

Using standard imaging pulse sequences, one can analyze the effects of blood flow on MR imaging in phantom studies (3, 5, 9, 10, 13, 14) or in patients with diseases showing slow flow (4, 7, 8). Alternatively, specially designed flow-sensitive pulse sequences can be tested in phantom studies (15, 16) or patients (6, 17). Although the latter approach will eventually make MR a versatile blood flow imaging modality, for practical reasons the former approach has been the only one available to most investigators.

The purpose of this paper is to examine and analyze some of the concepts relating to MR flow imaging and to apply these concepts to observations of intraluminal signal obtained in healthy subjects and patients with slow arterial flow, such as those with primary pulmonary arterial hypertension and low cardiac output. A special, so-called ECG-permutation triggered imaging technique was used in most patients; this permitted visualization of the same section at five different phases of the cardiac cycle starting at end diastole and extending throughout systole into early diastole (7, 8). Gated data acquisition is crucial when the highly pulsatile blood flow in the arterial system is imaged. In this presentation, emphasis is placed

¹ From the Departments of Radiology (G.K.v.S., C.B.H.), University of California, San Francisco and University Hospital (G.K.v.S.), Zurich, Switzerland. Received May 14, 1985; accepted and revision requested July 8; revision received July 24.

© RSNA, 1985

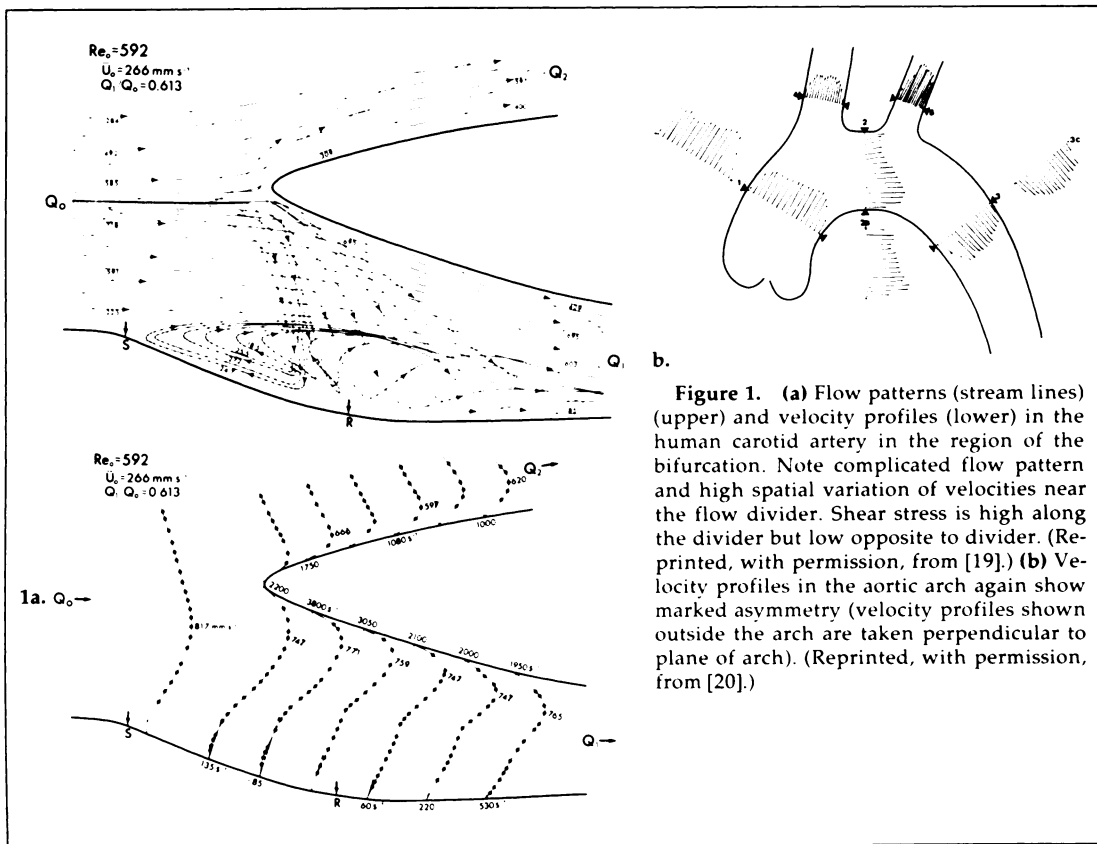


Figure 1. (a) Flow patterns (stream lines) (upper) and velocity profiles (lower) in the human carotid artery in the region of the bifurcation. Note complicated flow pattern and high spatial variation of velocities near the flow divider. Shear stress is high along the divider but low opposite to divider. (Reprinted, with permission, from [19].) (b) Velocity profiles in the aortic arch again show marked asymmetry (velocity profiles shown outside the arch are taken perpendicular to plane of arch). (Reprinted, with permission, from [20].)

on the notion that the *spatial* variation of the velocity of flowing blood within the imaged voxel is one of the major determining factors of intraluminal signal intensity, and that accelerated motion is also important in understanding blood flow phenomena in MR imaging.

CONCEPTS

Blood Flow in Vessels

A characteristic feature of fluid flowing in a vessel is the spatial variation of the velocity across the perfused lumen. This is different from the motion of solid tissue, such as the heart wall. Typically, the flow velocity is high in the center of the vessel, and it is always zero at the vessel walls. The fluid may exert considerable shear forces on these walls (12). Venous blood flow shows relatively weak cardiosynchronous changes and may assume a nearly parabolic velocity profile, consistent with laminar flow. Arterial blood flow, however, is highly pulsatile, with aortic peak velocities of 100–150 cm/sec in midsystole, dropping to virtually zero velocity in late diastole. Arterial blood flow has been termed “disturbed” flow to account for the fact that the terms “laminar” and “turbulent” flow are, strictly speaking, not applicable to the description of pulsatile flow (18). There is general agreement that arte-

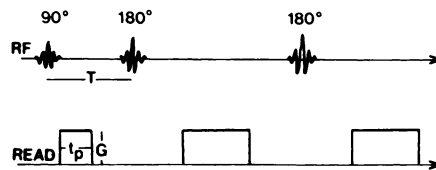


Figure 2. Spin-echo pulse sequence with two echoes (90°- nutation and two 180°-refocusing radiofrequency pulses). The readout gradient exhibits “balanced” properties, that is, the strength and duration of the gradient is symmetrical around the refocusing pulses. The long gradient pulses are exactly twice as long as the first pulse, and readout occurs in the middle of the long pulse.

rial flow has a pluglike, rather than a parabolic, velocity profile (18). Turbulent flow patterns are sometimes observed distal to vascular stenoses and may occur in aneurysms. Phantom studies of arterial blood flow show complicated flow patterns (19, 20), for example, at vascular bifurcations (Fig. 1a) and in curved vessels (Fig. 1b).

Not only the pulsatile cardiosynchronous variation of blood flow but also flow along curved vessels results in accelerated motion, because blood flowing through a bend loses velocity in one spatial direction and gains it in another. With accelerated motion taken into account, the position x of a moving spin at time t in a large blood vessel is described by the expression

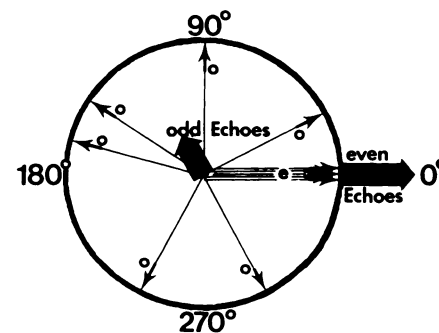


Figure 3. Circle on which spins precess after 90° nutation pulse. They all start out at zero degrees. Stationary spins will return to this position on each echo (spins labeled e). Spins moving at constant velocity will point in different directions on odd echoes (spins labeled o), their angle being proportional to their velocity, but will point in the zero degrees direction on even echoes (spins labeled e) (i.e. they refocus on even echoes). Accelerated spins will spread in proportion to their acceleration and the echo number (spins labeled a); no refocusing occurs at any echo.

$$x = x_0 + v_0 t + a_0 t^2 / 2 + (\text{higher-order terms}), \quad (1)$$

where x_0 , v_0 , and a_0 indicate the position, velocity, and acceleration, respectively, that exist at the time of the 90° nutation radiofrequency pulse, starting a spin-echo pulse sequence. Neglecting the higher-order terms in equation (1) is justified over the times relevant to spin-echo MR imaging (from the 90° pulse to the data acqui-

Table 1
Phase Angles for Stationary, Constant Velocity, and Accelerated Spins

180° Pulses and Echoes	Constant Position Phase shift Φ_3/b ($b = \gamma G_x x_0$)	Constant Velocity Phase Shift Φ_v/c ($c = \gamma G_x v_0/2$)	Constant Acceleration Phase Shift Φ_a/d ($d = \gamma G_x a_0/6$)
T	t_p	t_p^2	t_p^3
2T/first echo	0	$4Tt_p - 2t_p^2$	$12T^2t_p - 3Tt_p^2$
3T	t_p	$8Tt_p - t_p^2$	$24T^2t_p + t_p^3$
4T/second echo	0	0	$24T^2t_p - 6Tt_p^2$
5T	t_p	$8Tt_p + t_p^2$	$72T^2t_p + t_p^3$
6T/third echo	0	$4Tt_p - 2t_p^2$	$36T^2t_p - 9Tt_p^2$
7T	t_p	$16Tt_p - t_p^2$	$144T^2t_p + t_p^3$
8T/fourth echo	0	0	$48T^2t_p - 12Tt_p^2$
(2n + 1)T: (n-th refocusing pulse)			
n even	t_p	$4nTt_p + t_p^2$	$12(n^2 + n)T^2t_p + t_p^3$
n odd	t_p	$4(n + 1)Tt_p - t_p^2$	$12(n^2 + n)T^2t_p + t_p^3$
2nT: (n-th echo)			
n even	0	0	$12nT^2t_p - 3nTt_p^2$
n odd	0	$4Tt_p - t_p^2$	$12T^2t_p - 3nTt_p^2$

Note.— Φ = phase angle, γ = gyromagnetic ratio, x_0 = position, v_0 = velocity, a_0 = acceleration, G_x = magnetic gradient field strength along x direction, $T = \frac{1}{2}$ of spin-echo time TE, t_p = time interval during which gradient field is turned on.

sition), which are typically on the order of 100 msec. This is because, in humans, large acceleration changes are caused neither by the cardiosynchronous changes (typical cardiosynchronous variations occur over 300–400 msec that is length of systole) nor by blood vessel curvature (blood at peak velocity moves about 10 cm in 100 msec, a distance over which the large vessels in general exhibit no more than one directional change). Hence, over the time of a multiple spin-echo pulse sequence, the acceleration is approximately constant. This is equivalent to the statement that the higher-order terms of equation (1) may be neglected. Even in arterial blood flow, however, there are phases, such as during midsystole, when flow occurs at an approximately constant velocity over the time of a multiple spin-echo sequence, and acceleration effects are of minor importance.

MR Imaging of Moving Spins

Motion and flow affect MR imaging in two principal ways: by time-of-flight effects and by spin-phase change effects.

One type of time-of-flight effect is referred to as flow-related enhancement (5) and results from the motion of fully magnetized spins into the imaged volume at relatively low-flow velocities of a few centimeters per second between the nutation (90°) and the refocusing (180°) pulses of the imaging process. A second time-of-flight effect, termed high-velocity signal loss (5), occurs with relatively rapid flow (10 cm/sec or more), when spins flow out of the imaged volume

before the refocusing pulses occur. This effect may account for the fact that blood vessels usually show no signal when they course perpendicular to the imaging plane, but it cannot explain that vessels coursing within the imaged plane appear dark on MR images. Time-of-flight effects have been extensively analyzed (5, 7, 11, 21) and shall not be discussed further.

The second effect of motion on MR imaging results from spin-phase changes, which occur whenever spins move in gradient fields. As gradient fields are used for spatial position encoding, such effects occur in all imagers, but the signal produced by moving spins is in part imager specific. In contrast to time-of-flight effects, spin-phase changes also occur with motion within the imaged plane, because imaging gradients are present along all spatial coordinates at one or another time during an MR pulse sequence. The work presented here is concerned predominantly with such in-plane motion. The advantage of this restriction is that, for in-plane motion, time-of-flight effects (which are always associated with a motion component of spins perpendicular to the imaging section) do not enter into consideration, thus making an understanding of the observed phenomena simpler.

After a 90° nutation pulse (Fig. 2), the precessional phase of a spin, that is, the angle Φ through which a spin at a time-dependent position $x(t)$ in a gradient field has rotated compared with a stationary spin at a fixed position $x = 0$, is given by

$$d\Phi(t) = \gamma G_x(t)x(t)dt, \quad (2)$$

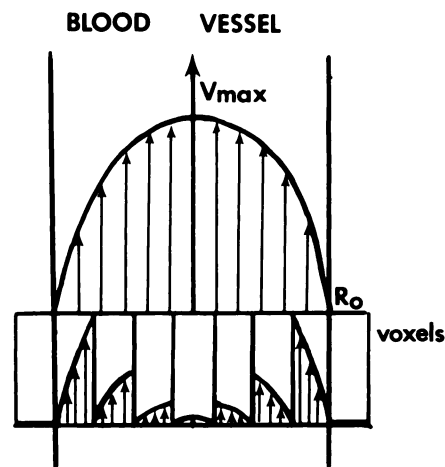


Figure 4. Hypothetical velocity profile across vessel lumen. Velocity is always zero at vessel wall. Below the profile, variation of velocities within individual voxels is shown. This variation is large close to the vessel wall and small in the center.

where $G_x(t)$ denotes the component of the gradient field along the x-axis, and γ is the gyromagnetic ratio (14). The same respective equations apply for the y- and z-axes. From equations (1) and (2), the phase of a spin undergoing any type of motion along the x axis can be calculated at any time after the nutation pulse, given the time span over which the gradient $G_x(t)$ is switched on. For a given multiple spin-echo sequence, where the gradient fields are switched on symmetrically around the refocusing pulses (Fig. 2) ("balanced" gradients), the results of such a calculation are summarized in Table 1 for spins at rest at x_0 , moving at a constant velocity v_0 , and at a constant acceleration a_0 . T in this table denotes the time between nutation (90°) and first refocusing (180°) pulse and equals half the echo time (TE). t_p is the time during which the gradient field is switched on (Fig. 2). We note in Table 1 that stationary spins will have zero phase, that is, return to their starting position on the phase circle at any echo. This is illustrated in Figure 3 by the spins labeled e . Spins moving at constant velocity v_0 , point in different directions on the phase circle (spins labeled o in Fig. 3) on odd echoes (1, 3, 5, etc.), the phase angle being proportional to v_0 , while they all point in the zero degree direction for even echoes (2, 4, 6, etc.). This phenomenon has been called "even-echo refocusing" or "rephasing" (17, 22). For purely accelerated motion, no such refocusing phenomena occur; that is, spins undergoing different accelerations will have different phase angles for any echo (spins labeled o in Fig. 3), and

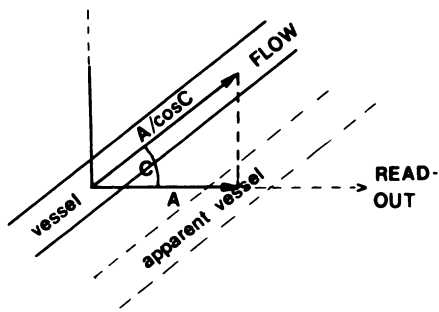


Figure 5. Spatial misregistration caused by flow. For oblique flow within imaging plane, phase encoding localizes spin position in the vertical direction right after 90° nutation pulse, but readout occurs after spins have moved a distance $A/\cos C$. Measuring the distance A of spatial misregistration and the angle C of the vessel to the horizontal permits one to estimate the flow velocity.

the gain in phase angle Φ is simply proportional to the acceleration a_0 and the echo number (Table 1). For a "balanced gradient" pulse sequence (Fig. 2), phase changes on odd echoes will be the result of constant velocity and accelerated motion. With even echoes, spin-phase changes are only a result of accelerated motion. Gradient pulse sequences other than the one shown in Figure 2 can be specifically designed to be sensitive to acceleration only (15.) For asymmetric pulse sequences, stationary spins will have a phase angle different from zero but will align along the same direction. Spins moving with differing constant velocities or accelerations, however, will not align, independent of whether the echo is odd or even.

Based on the preceding discussion, we may now understand why even blood vessels coursing within an imaged plane generally appear dark on spin-echo images. Figure 4 is a velocity profile across a vessel lumen. The velocity is always zero at the vessel wall and increases toward the center. Below the velocity profile, a hypothetical row of voxels is shown, together with the spatial velocity change within a voxel resulting from such a flow profile. This spatial velocity change is large toward the walls and gradually decreases toward the center of the vessel. The signal intensity for a given voxel in a blood vessel is the (vector) sum of the signals from all spins moving at different velocities. This leads to a situation, depicted in Figure 3 by the spins labeled o , where the resulting signal intensity per voxel is small on the first echo

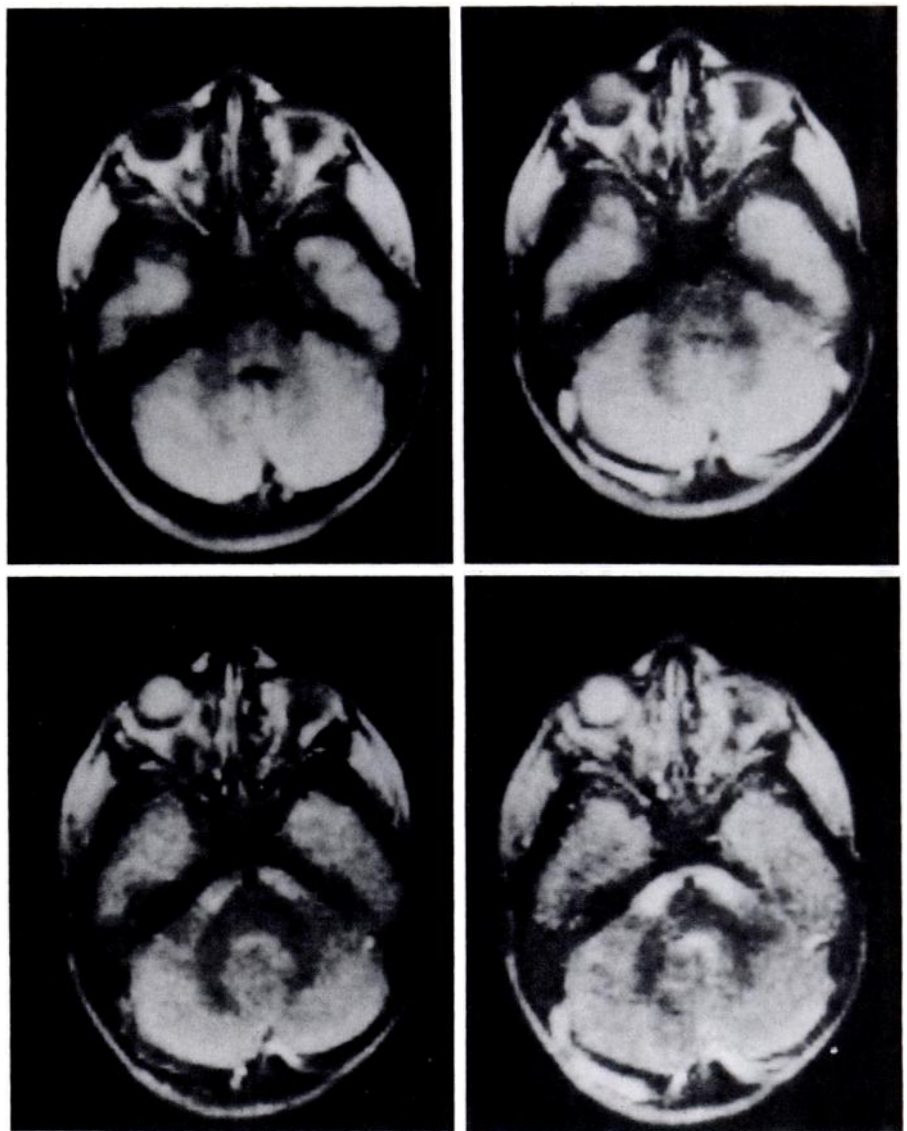


Figure 6. Four-echo transaxial study of a patient's head at the level of the transverse sinus. Note the presence of intraluminal signal, which is more prominent on even (second and fourth) echoes than on odd ones (first and third), representing even-echo refocusing.

(short bold arrow). For example, if the velocity difference between the two edges of a voxel is 1 cm/sec, this results in a spread of the signal vectors of the individual spins over almost the entire 360° for an MR imager such as the one used in our laboratory; this calculation can be made from the data in Table 1 with $\gamma = 2.7 \times 10^8 \text{ kg}^{-1}\text{secA}$, $G_x = 5 \times 10^{-4} \text{ T/cm}$, $t_p = 5 \times 10^{-3} \text{ sec}$, $T = 1.5 \times 10^{-2} \text{ sec}$. However, all spins moving at differing constant velocities will again point along the same direction on even echoes (arrows labeled e in Fig. 3). For an imager that shows rephasing phenomena along any spatial direction owing to balanced gradients (pulse sequence similar to that in Fig. 2). The resulting signal intensity is then high (long bold arrow). For spatial variations associated with accelerations within a voxel, the same type of spread-

ing of phases occurs (o spins in Fig. 3), but rephasing phenomena do not exist for balanced gradients (Table 1). Thus, the spins point in all different directions on the precession circle on odd as well as on even echoes.

We thus expect that signal loss occurs as the velocity and acceleration of blood in a vessel increase, because the respective velocity and acceleration profiles across the vessel become steeper. Signal loss should be most marked along the vessel wall or at vascular bends and bifurcations, where blood flow shows marked spatial variations in velocity and acceleration. For in-plane bulk motion, no signal loss occurs (in modulus images) because no significant velocity gradients exist across a voxel in solid tissue. This is amply illustrated by the appearance of the heart wall in gated MR studies. Signal loss owing to mi-

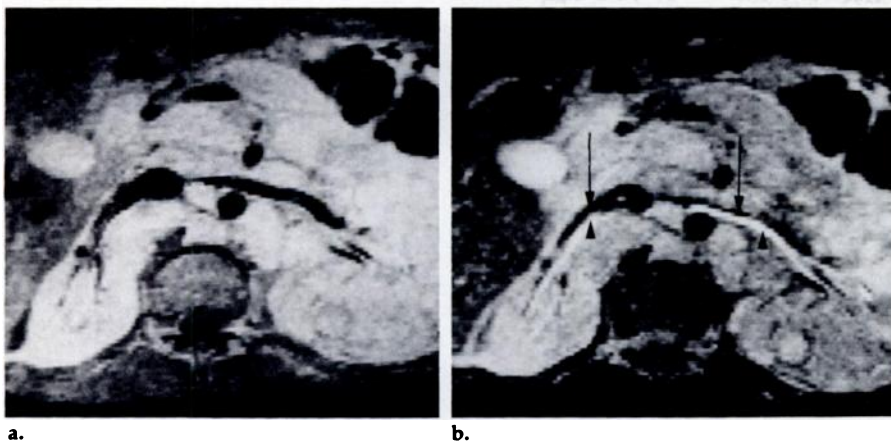


Figure 7. Even-echo refocusing and spatial misregistration in abdominal transaxial section of a patient with a left renal tumor. Note the medial displacement of the intraluminal flow signal in both renal veins (arrowheads) out of the anatomic confines of the vessels (arrows), resulting from medial flow of blood. **(a)** First-echo image. **(b)** Second-echo image.

crocirculatory flow in arterioles and venules can also be expected to occur in highly vascular tissues, such as the lung or the kidney. The small vessels in such tissues point in multiple directions and exhibit tortuosities over volumes the size of an imaging voxel. Provided that the gradient pulse sequences used result in phase changes on the order of 360° or more, even for small blood-flow velocities, the signal intensity within a voxel may again be reduced, but now because of the spins moving in small vessels that point in different directions.

Oblique In-plane Flow Misregistration

A second effect caused by spin-phase changes can be noted with in-plane flow on MR imaging. A spin moving obliquely within the plane of the phase-encoding and readout directions is phase encoded for a certain position shortly after the nutation (90°) pulse, but has moved to another position by the time readout occurs (Fig. 5). While such spins contribute signal at their actual position along the axis of the readout gradient (e. g., the horizontal axis), they appear at the position along the phase-encoding direction (e.g., along the vertical axis) where they were during phase encoding but have moved from at the time of signal readout. Thus they appear to be shifted outside the confines of a vessel coursing obliquely within the imaging plane (Fig. 5). Due to rephasing phenomena and longer echo-delay times, this spatial misregistration effect is seen more readily on even-echo images. In such instances, "conventional" MR imaging can yield information on the direction and approximate velocity of blood flow because the distance and the

time over which a spin travels along the readout axis and the angle of the readout axis to the vessel are known (Fig. 5).

The discussion of these concepts has focused on in-plane flow because, as stated above, time-of-flight phenomena have been discussed and are generally appreciated (5-7, 15, 21). This results in considerable conceptual simplification. Flow with a component perpendicular to the imaged section will also show effects based on spin-phase changes. The section-selection gradient, which is responsible for phase changes perpendicular to the imaged section, does not have the exact properties of symmetry shown for the readout gradient in Figure 2, and refocusing phenomena in such flow will only be partial. In this case, spins moving at a constant velocity are spread over the phase circle not only on odd echoes, but also, to a lesser degree, on even echoes. In addition, however, time-of-flight effects are important in determining the appearance of vessels coursing perpendicular to the imaging plane (5-7, 15, 21), and these effects vary depending on the direction of flow and multiple technical details of image acquisition.

PATIENTS AND METHODS

Images were acquired with a cryogenic MR imaging system, operating at a field strength of 0.35 T (Diasonics, Milpitas, Calif.). Most images were obtained from ECG-triggered studies. A permutation-gated sequence (7) was used in 18 patients. It yielded five dual-echo images at each of five adjacent levels (section thickness, 7 mm; 3-mm gap; pixel size, 1.7×1.7 mm) in the end-diastolic phase of the cardiac cycle (about 50-80 msec after onset of the QRS complex), in early, middle, and end systole (at about 150-180, 250-280, and 350-380 msec, respectively), and in early diastole

(at about 450-480 msec after the onset of the QRS complex). The readout gradient, which is symmetric around the refocusing (180°) pulses (Fig. 2), was applied in the horizontal direction during transverse imaging (x-axis) and along the main magnetic field (z-axis) during sagittal and coronal imaging. The section-selection gradient was along the z-axis during transverse, along the horizontal x-axis during sagittal, and along the vertical y-axis during coronal imaging. Quantitative analysis of pixel intensity profiles across vascular lumina was done in four cases.

Because our imager was not equipped with pulse sequences specifically designed for flow imaging, patients had to be selected such that intravascular signal was observable in at least part of the cardiac cycle and in part of the vascular lumen. The illustrations presented here were selected from those of healthy volunteers ($n = 6$), patients with pulmonary arterial hypertension ($n = 10$), low cardiac output syndromes ($n = 4$), and patients with various other disease states ($n = 30$). Studies of the arteries were limited to the mediastinum because of the size of the vessels. This resulted in many voxels within the cross section of a vessel.

CLINICAL APPLICATIONS

Veins: Constant Velocity Flow Phenomena

Slow, in-plane flow conditions with nearly constant velocity in transaxial images occur in both healthy and unhealthy subjects. They are predominantly seen in the transverse sinuses of the brain and the hepatic and renal veins, which are oriented in such planes. Figure 6 shows a four spin-echo sequence with slow flow in the transverse sinuses. Reduced signal intensity in the sinuses is observed on the first and third (odd) echoes compared with the second and fourth (even) echoes. This is an example of even-echo refocusing, frequently seen on MR images.

Even-echo intravascular signal is also commonly noted in the upper abdomen. Figure 7 is an example of second-echo refocusing in the renal veins in a patient with a left renal and retroperitoneal tumor. Comparison of first- and second-echo images show that the second-echo flow signal, in this case, is displaced in a medial direction out of the anatomic confines of both renal veins, consistent with a medial flow direction in these vessels. This is an example of oblique in-plane flow misregistration, which was schematically illustrated in Figure 5.

Arteries: Pulsatile Blood Flow

Examination of flow phenomena in the arterial system requires cardiac triggering. All images presented in

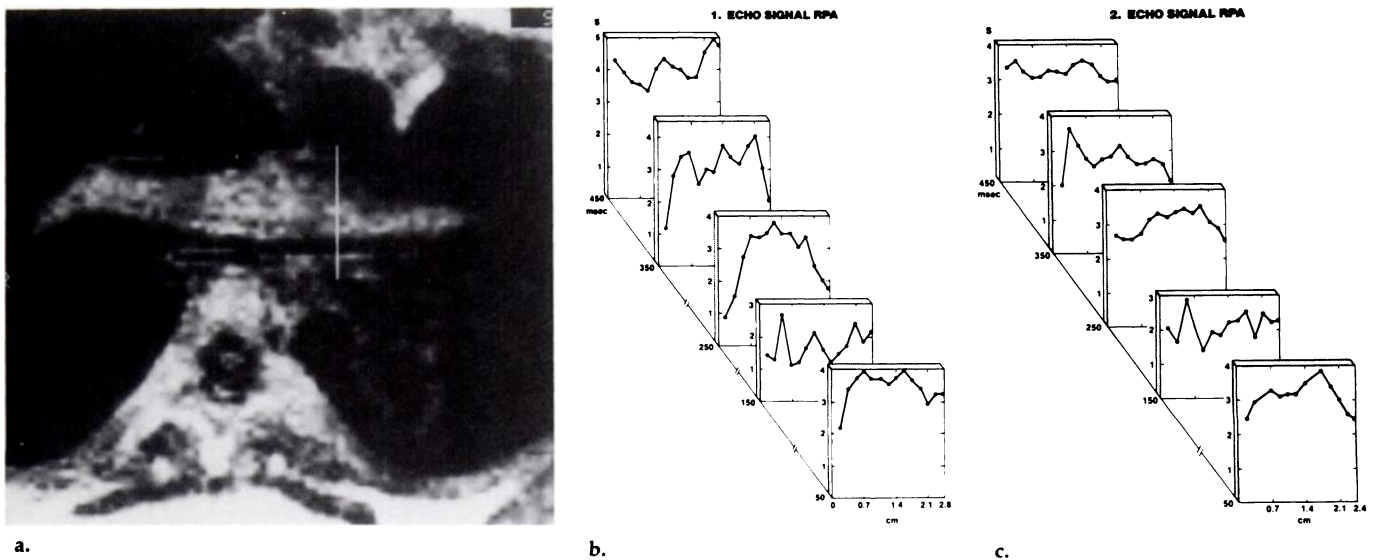


Figure 8. (a) Mid-systolic intraluminal flow signal on ECG-gated first-echo image of a patient with pulmonary hypertension. Note signal loss along vessel walls of right pulmonary artery. The cross-sectional line indicates where intensity profiles were measured. (b) First- and (c) second-echo intensity profiles across right pulmonary artery in the same patient taken at five different phases of the cardiac cycle.

this section were acquired in this fashion. Figure 8a demonstrates mid-systolic slow flow in the pulmonary arteries of a patient with primary pulmonary hypertension (PAH) on a first-echo image. In this axial image, flow in the right pulmonary artery (RPA) occurs along the direction of the readout gradient. Along the cross section of the RPA in Figure 8a, the pixel by pixel absolute signal intensity was obtained for all five first- and second-echo images at this level during the different cardiac phases. In Figure 8b and 8c, the cross-sectional intensities for all images are presented (vessel diameter, 2.5 cm). At end diastole (50 msec), the signal intensity was nearly constant across the RPA and similar on the first and second echoes. This is the result of the slow flow occurring in the RPA during end diastole, resulting in slight velocity differences within voxels and thus some first-echo signal loss. The second panels (150 msec) in Figure 8b and 8c show the RPA intensity profile during early systole, where blood was rapidly accelerated from almost zero velocity to velocities of several tens of centimeters per second. A decrease in signal intensity was noted for both first- and second-echo profiles, consistent with the notion that signal loss occurs for all echoes when the motion is predominantly accelerated (Table 1). In midsystole (250 msec), a flow pattern with nearly constant velocity had been established, which showed signal loss on first echo along the vessel wall (Fig. 8a), as reflected in the intensity profile on the corresponding panel of Figure 8b. This signal loss is a result of the spatial velocity changes with zero flow velocity at the

vessel wall, but velocities of 10 cm/sec or more just 1-2 mm away from the wall (Fig. 4). Since there are little changes in acceleration during the midsystolic phase of the cardiac cycle, the acceleration profile across the RPA was essentially equal to zero. Acceleration-induced signal loss, which would show on the second-echo image, was therefore not observed. This also explains why signal was present along the vessel wall on the second-echo intensity profile in contrast to the first-echo intensity profile (Fig. 8b, 8c; panel at 250 msec). During the end systolic and early diastolic phases of the cardiac cycle, the flow of blood in the RPA gradually subsided, resulting in a renewed increase in intravascular signal intensity (Fig. 8b, 8c; panels at 350 and 450 msec).

Similar effects were observed in the descending aorta in patients with low cardiac output and in late systolic and early diastolic images of healthy subjects where blood flow is slow. Note that in sagittal images, the readout gradient approximately parallels the direction of the descending aorta. In Figure 9, midsystolic first- and second-echo images of a patient with low cardiac output are shown. Note again the first-echo signal loss along the wall of the descending aorta and the aortic arch. The second-echo image also showed signal loss along the wall, but it was less pronounced. The signal loss in the aortic arch region is a result of flow in a curved vessel, where the directional change in blood flow not only produces accelerated motion of flow in the plane of the arch (Fig. 1b) but also induces a circular flow pattern close to the aor-

tic wall (18, 20). These circular motions persist for some distance into the straight segment of the descending aorta, hence signal loss along the vessel wall also occurs on the second-echo image.

Figure 10 is another example of the influence of spatial velocity and acceleration variations on signal intensity across the vascular lumen. Signal loss occurred asymmetrically along the vessel wall, suggesting that the flow around the 90° turn resulted in an asymmetric velocity and acceleration profile across the vascular lumen (Fig. 1b)(18-20). Asymmetric intravascular signal loss could also be observed at vascular bifurcations, where the spatial velocity and acceleration changes next to the crotch of the bifurcation are higher than at the vessel walls opposite the crotch (Fig. 1a)(19). Figure 11 shows an example of this phenomenon in a patient with PAH.

While blood flow with a component perpendicular to the imaged section showed less prominent refocusing phenomena owing to a lack of symmetry of the section-selection gradient around the refocusing pulses, signal loss owing to significant velocity changes near the vessel wall also occurred. This is exemplified by a midsystolic transaxial image containing the descending aorta (Fig. 12a) of a patient with low cardiac output. The corresponding first-echo intensity profile across a vertical central section is shown in Figure 12b. Note the rim of low signal intensity around the high central signal in the first-echo image. Since this image was the second to last section in a multisec-tion study, the dark ring on this image cannot be the result of time-of-

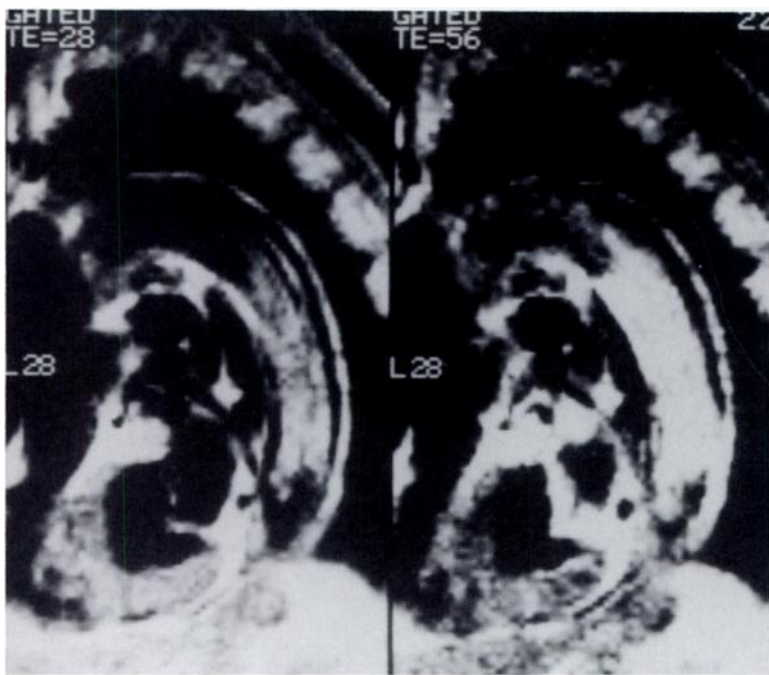


Figure 9. Sagittal midsystolic image of a patient with low cardiac output showing signal inside the aorta. Signal loss occurs along the vessel wall and in the aortic arch, more prominently on first- than on second-echo image.

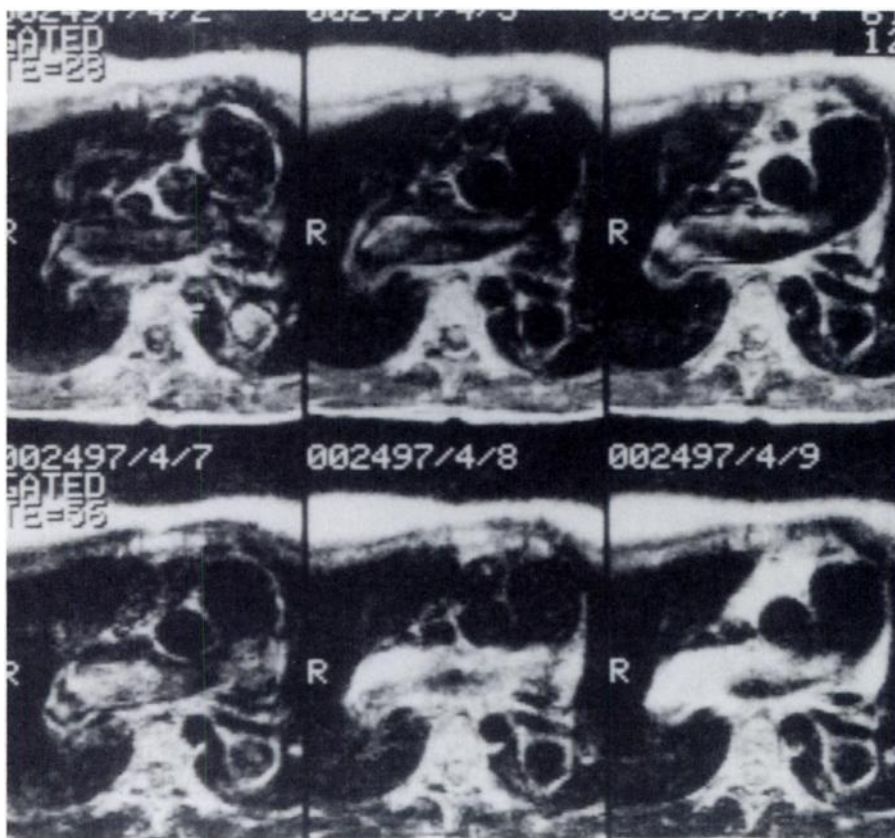


Figure 10. Composite of three first-echo images (top row) and three second-echo images (bottom row) through the right pulmonary artery in a patient with pulmonary arterial hypertension, taken during early, middle, and end systole. Note the variability in signal distribution across vascular lumen, suggesting higher spatial velocity changes along the outside of the vessel.

flight phenomena. These latter phenomena can also produce dark rings that increase in size for sections further into the stack of a multisection study and are seen with se-

quences employing short repetition times (5). No signal was present on the second-echo image (as well as the third- and fourth-echo images, not shown here). This is a result of time-

of-flight effects; a considerable number of the protons that have undergone the 90° - nutation pulse still contribute signal during the first 180° - refocusing pulse but have left the section before the second and further 180° - refocusing pulses occur. In fact, the slight central drop of first-echo signal intensity, best appreciated in the intensity profile of Figure 12b, indicates that in the most central portion of the vessel, where blood flow is fastest, high-velocity signal loss owing to section transition of spins becomes operative even on the first echo. Finally, Figure 13 shows a transaxial section through the liver (23). The portal veins, which are in-plane in this image, show high signal intensity on the second-echo (refocusing) image, while the hepatic veins, running perpendicular to the section, show no signal as a result of section transition effects.

Inclusion of time-of-flight effects in the analysis of flow phenomena in MR imaging is important in many cases where one component of the flow is perpendicular to the imaged section, but it complicates such an analysis considerably.

Small Vessels and Microvasculature

Preliminary observations suggest that the flow in small arteries and arterioles, which is also pulsatile and cardiosynchronous, affects the observed signal intensity from the peripheral lung fields (8). An illustration of this is Figure 14, where first-echo end-diastolic and midsystolic images of a healthy volunteer, taken at the same axial level, are shown. Vessels are seen to radiate peripherally from the pulmonary hila in end diastole, while these vessels are not apparent during end systole. This again suggests signal loss caused by flow and resulting spatial velocity variations within the voxels containing these vessels. Furthermore, the peripheral lung tissues have higher signal intensity during end diastole than during systole. Rather than being the result of velocity differences across the lumina of vessels, this signal loss could be due to blood flowing through the small peripheral vessels with their wide range of spatial orientations within a voxel (8). If the increase in signal intensity were simply the result of an increase in the pulmonary blood pool, higher signal inten-

Figures 11-14 are on p. 694.

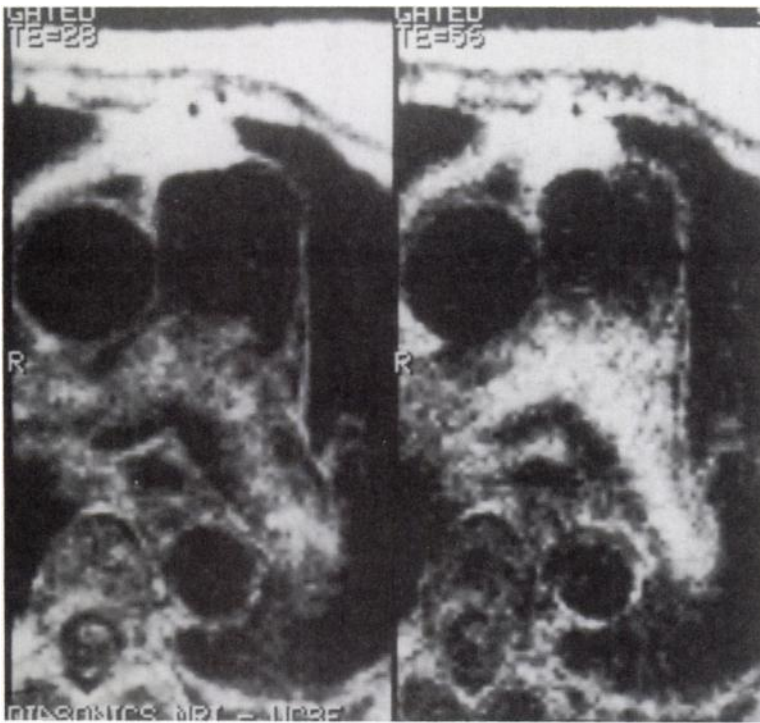


Figure 11. Signal loss at the crotch of the bifurcation of the main pulmonary artery on first-echo (left) and second-echo (right) images in a patient with pulmonary arterial hypertension.

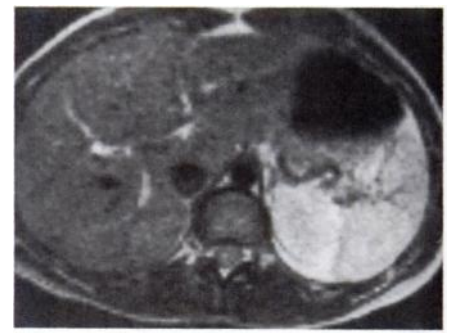


Figure 13. Transaxial second-echo image through liver showing high signal intensity in the portal veins, which predominantly course parallel to the plane of section at this anatomic level, but no signal in hepatic veins, which run more perpendicular to imaging plane. (Reproduced, with permission, from [23].)

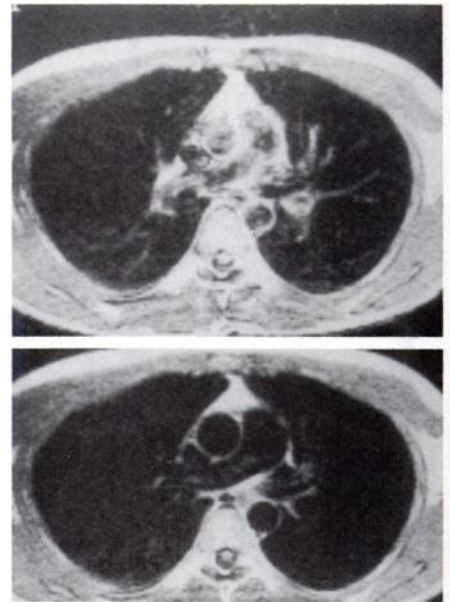
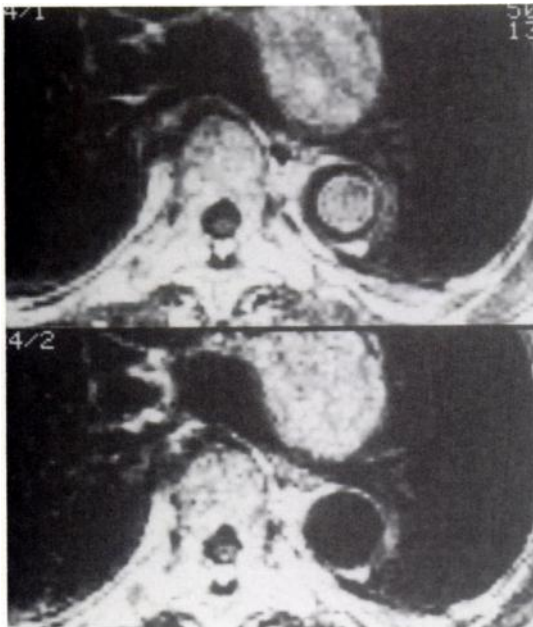


Figure 14. End-diastolic (top) and mid-systolic (bottom) first-echo images in a healthy volunteer at the level of the pulmonary arteries. On the end-diastolic image, the pulmonary vasculature extending into the lung parenchyma is noted, while in midsystole, these vessels are not seen. Furthermore, there is an overall decrease in signal intensity in the peripheral lung fields in midsystole compared with the end-diastolic image.



a.

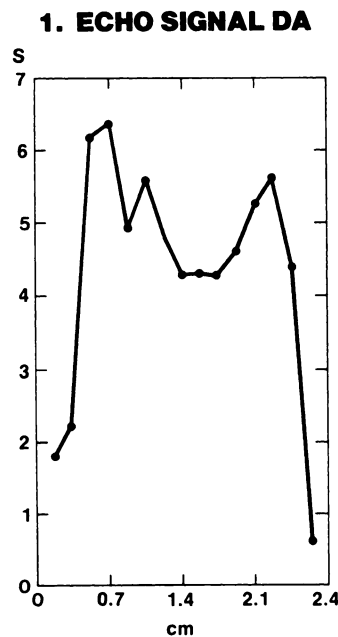


Figure 12. (a) First-echo (top) and second-echo (bottom) transaxial images of the descending aorta in a patient with low cardiac output. Note rim of signal loss combined with some decrease of signal in center of vessel on first echo, but complete signal loss on second echo. (b) Signal intensity profile across the lumen. There is signal loss along vessel wall, as well as some central signal loss.

sity would actually be expected during systole (24).

CONCLUSION

Current MR imagers show two major types of flow effects: time-of-flight and spin-phase change effects owing to motion of spins in gradient fields.

For in-plane flow, only the second type of effect is relevant, thus simplifying the analysis of flow phenomena. During time intervals relevant to spin-echo (and inversion-recovery spin-echo) sequences (about 100 msec), constant velocity and acceleration predominantly determine the signal from blood vessels coursing

within the imaging plane. The signal intensity from vessels is critically dependent on the spatial distribution of velocities and accelerations (velocity and acceleration profiles) within a voxel. This spatial distribution is, in turn, a function of the dimensions of the vessel and the average flow velocity and acceleration. The larger the spatial variation of the velocity or acceleration across a voxel, the greater the loss in signal amplitude in MR imaging. With balanced gradients, which are characteristic of the read-out gradient, refocusing phenomena

occur, which make the even-echo images sensitive to signal loss by accelerated flow only, whereas odd echoes show signal loss owing to both velocity and acceleration. Both odd and even echoes are sensitive to velocity and acceleration for flow along non-symmetrical gradients, typified by the section-selection and phase-encoding gradients. Signal loss owing to spin-phase changes can be observed in veins, in arteries of healthy subjects during the diastolic phases of the cardiac cycle and patients with disease states causing slow flow, and possibly in the microvasculature of the lung. Recognition of such effects in MR imaging is of importance in the differentiation between venous or arterial slow flow and thrombus (25) and can be used as an adjunct in the diagnosis of pathologic conditions in the cardiovascular system (7, 8). Potential future applications include the identification of regions of increased shear forces on arterial walls, which are thought to be a cause of atherosclerosis (12). Such shear forces are closely related to spatial velocity and acceleration changes along the arterial walls, and these changes can be recognized *directly* by loss of signal intensity on MR images. Preliminary results also indicate that flow in the microvasculature reduces signal intensity from the peripheral lung fields (8). Thus, MR imaging may have a future role in the assessment of tissue perfusion, which is essential for the measurement of ischemic disease and pulmonary embolism. ■

Send correspondence and reprint requests to: Gustav K. von Schulthess, M.D., Ph.D., Depart-

ment of Radiology, University Hospital, CH-8091 Zurich, Switzerland.

References

- Hahn EL. Detection of sea water motion by nuclear precession. *J Geophys Res* 1960; 65:776-777.
- Moran PR. A flow velocity zeugmatographic interlace for NMR imaging in humans. *Magn Reson Imaging* 1982; 1:197-203.
- George CR, Jacobs G, McIntyre WJ, et al. Magnetic resonance signal intensity patterns obtained from continuous and pulsatile flow models. *Radiology* 1984; 151:421-428.
- van Dijk P. Direct cardiac NMR imaging of heart wall and blood flow velocity. *J Comput Assist Tomogr* 1984; 8:429-436.
- Bradley WG, Waluch V. Blood flow: magnetic resonance imaging. *Radiology* 1985; 154:443-450.
- Singer JR, Crooks LE. Nuclear magnetic resonance blood flow measurements in the human brain. *Science* 1983; 221:654-656.
- von Schulthess GK, Fisher MR, Crooks LE, Higgins CB. Gated MR imaging of the heart: intracardiac signals in patients and healthy subjects. *Radiology* 1985; 156:125-132.
- von Schulthess GK, Fisher MR, Higgins CB. Pathologic blood flow in pulmonary vascular disease as shown by gated magnetic resonance imaging. *Ann Intern Med* 1985; 103:317-323.
- Bryant DJ, Payne JA, Firmin DN, Longmore DB. Measurement of flow with NMR imaging using a gradient pulse and phase difference technique. *J Comput Assist Tomogr* 1984; 8:588-593.
- O'Donnell M. NMR blood flow imaging using multiecho phase contrast sequences. *Med Phys* 1985; 12:59-64.
- Wehrli FW, McFall JR, Shutts D, Glover GH, Herfkens RJ. Approaches to in-plane and out-of-plane flow imaging. *Noninvasive Med Imaging* 1984; 1:127-136.
- Schettler RM, Nerem RM, Schmid-Schönbein H, Mörl H, Diehm C. Fluid dynamics as a localizing factor for atherosclerosis. Proceedings of a symposium held at Heidelberg, FRG, June 18-20, 1982. Springer Berlin.
- Bradley WG, Waluch V, Lai KS, Fernandez EJ, Spalter C. The appearance of rapidly flowing blood on magnetic resonance images. *AJR* 1984; 143:1157-1174.
- Wehrli FW, Shimakawa A, McFall JR, Axel L, Perman W. MR imaging of venous and arterial flow by a selective saturation-recovery spin-echo method. *J Comput Assist Tomogr* 1985; 9:537-545.
- Moran PR, Moran RA. Imaging true velocity and higher order motion quantities by phase gradient modulation techniques in NMR scanners. In: Esser BD, Johnston RE, eds. *Techniques of NMR imaging*. New York: Society of Nuclear Medicine, 1984.
- Moran PR, Moran RA, Karstaedt RA. Verification and evaluation of internal flow and motion. *Radiology* 1985; 154:433-441.
- Feinberg DA, Crooks LE, Hoenninger J, Arakawa M, Watts J. Pulsatile blood flow velocity in human arteries displayed by magnetic resonance imaging. *Radiology* 1984; 153:177-180.
- McDonald DA. *Blood flow in arteries*. 2d ed. Baltimore: Williams & Wilkins, 1974.
- Motomiya M, Karino T. Flow patterns in the human carotid artery. *Stroke* 1984; 15:50-56.
- Farthing SP, Peronneau P. Flow in the thoracic aorta. *Cardiovasc Res* 1979; 13:607-620.
- Crooks LE, Mills CM, Davis PL, et al. Visualization of cerebral and vascular abnormalities by NMR imaging. The effects of imaging parameters on contrast. *Radiology* 1982; 144:843-854.
- Bradley WG, Waluch V. NMR even echo rephasing in slow laminar flow. *J Comput Assist Tomogr* 1984; 8:594-598.
- Fisher MR, Wall SD, Hricak H, McCarthy S, Kerlan RK. Hepatic vascular anatomy on magnetic resonance imaging. *AJR* 1985; 144:739-746.
- Okada RD, Pohost GM, Kirschenbaum HD, et al. Radionuclide-determined change in pulmonary blood volume with exercise improved sensitivity of multigated blood pool scanning in detecting coronary artery disease. *N Engl J Med* 1979; 301:569-573.
- Fisher ME, Higgins CB. Central thrombi in pulmonary arterial hypertension: detection using MR imaging. *Radiology* (in press).